DOI: 10.1002/zaac.201300011

Syntheses, Structures, and Properties of Three Metal-Organic Complexes with Different Dimensionality Based on Dipyrido[3,2-d:2′3′-f]quinoxaline and Different Dicarboxylates

Xiu-Li Wang,*[a] Yun Qu,[a] Guo-Cheng Liu,[a] Jing-Jing Huang,[a] and Hong-Yan Lin[a]

Keywords: Lead; Nickel; Phenanthroline derivatives; Organic dicarboxylates; Crystal structure; Luminescence

Abstract. Three new metal-organic complexes $[Ni_2(dpq)_2(L^1)_2(H_2O)_5]\cdot H_2O$ (**1**), $[Pb_2(dpq)_2(L^1)_2]\cdot H_2O$ (**2**), and $[Pb(dpq)(L^2)]$ (**3**) (dpq = dipyrido[3,2-d:2′3′-f]quinoxaline, H_2L^1 = 1,1′-biphenyl-2,2′-dicarboxylic acid, H_2L^2 = 2-carboxymethylsulfanyl nicotinic acid) were synthesized under hydrothermal conditions and structurally characterized by elemental analyses, IR, and single-crystal X-ray diffraction analyses. X-ray analysis reveals that complex **1** has a semi-cycling dinuclear unit, which is extended into a 3D supramolecular architecture by hydrogen bonding and π–π stacking interactions. Complex **2** is an unusual 0D + 1D cocrystal of dinuclear units and left-/right-handed helical chains, which are ultimately packed into a 3D supramolecular structure through hydrogen bonding interactions. Complex **3** shows a 2D network bridged by L^2 anions, which is finally extended into a 3D supramolecular structure through π–π stacking interactions. The diverse structures of complexes **1**–**3** indicate that the central metal ions and the dicarboxylates have significant effects on the final structures. Moreover, the thermal stabilities, the photoluminescent properties of complexes **1**–**3** and the electrochemical property of complex **1** were also investigated.

Introduction

The past decade has seen remarkable progress in the development of new materials based on metal ions and organic ligands, often termed as metal-organic complexes (MOCs).[1] These MOCs can be synthesized and tuned by a suitable choice of the properties of the organic ligands, such as shape, functionality, flexibility, symmetry, length, and substituent group, as well as the properties of central metal ions, such as radius, valence electron, and coordination ability[2–6]. However, the rational design and assembly of prospective MOCs with unique structures and specific functions still remain a great challenge.[7,8] The N-donor ligands have been intensely investigated for the construction of new MOCs, because they can satisfy and even mediate the coordination needs of the central metal atoms and consequently generate more meaningful architectures.[9] To the best of our knowledge, however, the employment of rigid phenanthroline derivatives in the MOCs is relatively limited.[10] In addition, as an important family of multidentate O-donor ligands, organic dicarboxylates as bridging ligands seem to be excellent building blocks with versatile coordination modes and strong coordination capability for constructing high-dimensional architectures with interesting properties, and they also can be used as hydrogen-bond acceptors and donors in the construction of supramolecular frameworks.[11,12]

On the basis of the aforementioned points, in this work, we selected a chelating phenanthroline derivative dipyrido[3,2-d:2′3′-f]quinoxaline (dpq) as the main ligand, two kinds of dicarboxylic acids [1,1′-biphenyl-2,2′-dicarboxylic acid (H_2L^1) and 2-carboxymethylsulfanyl nicotinic acid (H_2L^2)] as the secondary ligands (Scheme 1) to react with metal Ni^{II} and Pb^{II} ions, aiming at investigating the effect of central ions and dicarboxylates on the target MOCs. The selection of dpq, H_2L^1, and H_2L^2 is basing on the following consideration: (a) dpq has large aromatic-ring system and may provide potential supramolecular recognition sites for π–π aromatic stacking interactions except for its strong coordination ability;[13–15] (b) The H_2L^1 ligand contains two bridging carboxyl groups, which can lead to a variety of connection modes with central metal atoms and provides abundant structural motifs.[16] Moreover, the distortion of the diphenyl spacer endows H_2L^1 a peculiar characterization to link metal ions or metal clusters into macrocycles or helical chains;[17] (c) H_2L^2 is a fantastic semi-rigid O-containing ligand with potential versatile coordination behavior, which has one rigid carboxyl group (–COOH) and one flexible S-containing building unit (–SCH_2COOH).[18]

As a result, three new metal-organic complexes $[Ni_2(dpq)_2(L^1)_2(H_2O)_5]\cdot H_2O$ (**1**), $[Pb_2(dpq)_2(L^1)_2]\cdot H_2O$ (**2**), and $[Pb(dpq)(L^2)]$ (**3**) were synthesized under hydrothermal conditions. In addition, the luminescent properties of the complexes **1**–**3** and electrochemical behavior of complex **1** in the solid state were investigated.

* Prof. Dr. X.-L. Wang
E-Mail: wangxiuli@bhu.edu.cn
[a] Department of Chemistry
Liaoning Province Silicon Materials Engineering Technology Research Centre
Bohai University
Jinzhou 121000, P. R. China

Supporting information for this article is available on the WWW under **http://dx.doi.org/10.1002/zaac.201300011** or from the author.

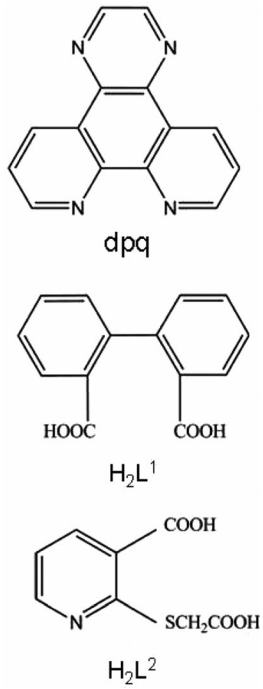

Scheme 1. Three types of ligands in this paper.

Results and Discussion

Description of Crystal Structures

*Structural Analysis of $[Ni_2(dpq)_2(L^1)_2(H_2O)_5]\cdot H_2O$ (**1**)*

Single crystal X-ray analysis shows that complex **1** is a 3D supramolecular architecture constructed from dinuclear units exhibiting a semi-circling feature. As shown in Figure 1a, two crystallographically independent nickel ions exhibit same octahedral coordination arrangements and the L^1 anions show the monodentate (L^1_a) and bridging-bis(monodentate) coordination modes (L^1_b) in complex **1**. The Ni(1) ion in the dinuclear complex is coordinated by one oxygen atom from a carboxyl group of one L^1_b anion [Ni–O bond length 2.052(2) Å], three oxygen atoms from three coordinated water molecules [Ni–O bond lengths 2.060(2), 2.070(2), and 2.043(2) Å] and two nitrogen atoms from a chelating dpq ligand [Ni–N = 2.087(2) and 2.079(2) Å], showing an octahedral arrangement. The Ni(2) atom is also six-coordinate by two oxygen atoms from different carboxyl groups of L^1_a and L^1_b [Ni–O = 2.061(2) and 2.060(2) Å], two oxygen atoms from two coordinated water molecules [Ni–O = 2.081(2) and 2.077(2) Å] and two nitrogen atoms from a chelating dpq ligand [Ni–N = 2.055(3) and 2.104(3) Å].

Two types of hydrogen bonding interactions between the oxygen atoms of lattice water molecules and carboxyl groups of L^1 [O(6W)–H(6WB)···O(6), 2.776(5) Å] and the carbon atoms of dpq ligands [O(6W)–H(38A)···C(38), 3.302(5) Å] connect the dinuclear units into 1D chain-A (Figure 1b). The hydrogen bonding interactions between the oxygen atoms of coordination water molecules and the carboxyl groups from L_a anions [O(3W)–H(3WB)···O(8), O···O distance is 2.747(4) Å], as well as the nitrogen atoms of dpq ligands and the carbon atoms of L^1 anions [C(23)–H(23A)···N(7), C···N distance is 3.460(5) Å] bridge the dinuclear motifs into 1D chain-B (Figure 1c). Finally, these two 1D supramolecular chains are further extended into 3D supramolecular framework through π–π stacking interactions between the aromatic rings of dpq ligands with centroid-to-centroid distances of 3.704 and 3.717 Å (Figure 1d).

In this complex, Ni(1) and Ni(2) ions are bridged by a L^1_b anion via coordination bonds forming a semi-cycling unit, whereas the L^1_a anion connects Ni(1) and Ni(2) ions by two types of interactions: Ni–O coordination bond and the hydrogen bonding interactions between the oxygen atom of carboxyl groups from L^1 anions and the coordination water molecules [O(4W)–H(4WB)···O(7), 2.783(3) Å, O(2W)–H(2WB)···O(5),

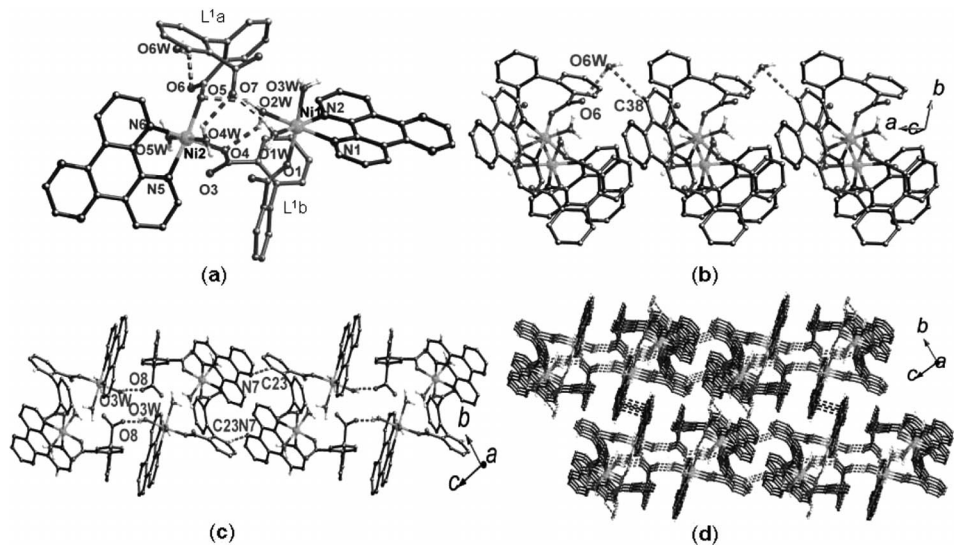

Figure 1. (a) Coordination environment for Ni^{II} ions in complex **1**. (b) 1D chain-A extended by hydrogen bonding interactions. (c) 1D chain-B linked by hydrogen bonding interactions. (d) 3D supramolecular structure connected by hydrogen bonding and π–π stacking interactions.

Zeitschrift für anorganische und allgemeine Chemie ZAAC Journal of Inorganic and General Chemistry

3.043(3) Å]. *Wang* and co-workers have reported a dinuclear Cd^{II} complex $[Cd_2(L^1)_2(phen)_2(H_2O)_2]$ and our group has synthesized a dinuclear Zn^{II} complex $[Zn_2(bdc)_2(dpq)_2]\cdot H_2O$ (bdc = benzene-1,2-dicarboxylate).[19,20] In these two dinuclear complexes, both of the carboxyl groups of the carboxylates coordinate with two central metal atoms forming circling dinuclear complexes, which are different from the semi-circling dinuclear complex **1**.

*Structural Analysis of $[Pb_2(dpq)_2(L^1)_2]\cdot H_2O$ (**2**)*

X-ray diffraction analysis reveals that complex **2** is a 3D supramolecular network derived from 1D left-/right-handed helical chains and dinuclear Pb^{II} units. The coordination environment of Pb^{II} ions is shown in Figure 2a. There are two crystallographically independent Pb^{II} ions. The Pb1 atom is coordinated by four oxygen atoms from two carboxyl groups of two L^1 anions [Pb–O distances range from 2.489(5) to 2.683(5) Å] and two nitrogen atoms belonging to one chelating dpq ligand with bond lengths of 2.668(5) Å [Pb1–N1] and 2.579(5) Å [Pb1–N2]. Two Pb1 ions are connected by two L^1 anions to form a circling dinuclear unit with the Pb···Pb distance of 6.1892 Å, in which the L^1 anions adopt a chelating bidentate bridging coordination mode. The Pb2 atom is also coordinated by two nitrogen atoms from one chelating dpq ligand with bond lengths of 2.684(5) Å [Pb2–N5] and 2.680(5) Å [Pb2–N6] and four oxygen atoms from two carboxyl groups of two L^1 anions [Pb–O distances range from 2.372(4) to 2.702(5) Å]. Adjacent Pb2 ions are connected by bridging L^1 anions to form 1D helical chain with a Pb···Pb distance of 8.2853 Å. The 1D helical chain is linked by adjacent another 1D helical chain through hydrogen bonding interactions to form a 1D double chains [O(5)–H(29A)···C(29), 3.134(4) Å]. The adjacent double chains are further connected by the dinuclear Pb1 units through hydrogen bonding interactions [O(1W)–H(1WB)···O(8), 2.762(8) Å and O(1W)–H(4A)···C(4), 3.384(2) Å], giving rise to a 2D supramolecular network (Figure 2b). The 2D networks are ultimately packed into a 3D supramolecular structure through hydrogen bonding interactions [O(1W)–H(15A)···C(15), 3.208(4) Å] (Figure 2c).

Interestingly, complex **2** is a novel 0D + 1D cocrystal of dinuclear units and the left- / right-handed helical chains. *Gao* and co-workers have obtained an interesting cocrystal of dinuclear motifs $[Zn_2(bta)_2(NH_3)_2]$ and 1D zigzag chains $[Zn(bta)(NH_3)_2]_n$ [bta = bis(5-tetrazolyl)amine].[21] In our previous work, we have reported a 0D + 1D cocrystal of dinuclear motifs $[Cd_2(dpq)_2(1,8\text{-ndc})_2]$ and 1D left- and right-handed helical chains $[Cd(dpq)(1,8\text{-ndc})_2]_n$ (1,8-ndc = 1,8-naphthalenedicarboxylate).[22] In these cocrystal complexes, complex **2** is the first example derived from dpq and main group metal.

*Structural Analysis of $[Pb(dpq)(L^2)]$ (**3**)*

Complex **3** exhibits a 2D polymeric layer structure, which was extended into a 3D network by supramolecular interactions. The Pb1 atom is seven-coordinated by two nitrogen atoms from one dpq ligand, five oxygen atoms from two chelating and one bridging carboxyl groups of three different L^2 anions with Pb–O distances ranging from 2.460(4) to 2.690(3) Å, as shown in Figure 3a. The dpq ligand acts as a typical chelating ligand terminally coordinating to the Pb1 with the Pb–N distances of 2.687(4) (Pb1–N1) and 2.676(4) (Pb1–N2), respectively. The two carboxyl groups of L^2 anion show two different coordination modes. One adopts the chelate coordination mode (type I), and the other exhibits chelate-monodentate bridging coordination mode (type II). The adjacent Pb^{II} ions are bridged by the two carboxyl groups of L^2 anions with type I and type II modes to generate a 2D layer (Figure 3b). The dpq ligands are attached to both sides of the layer. Finally, the 2D layer are extended by π–π stacking interactions between the pyrazine (N3) and coordinated pyridyl (N2) rings of dpq ligands from adjacent layers into a 3D supramolecular architecture (with a face-to-face distance of ca. 3.342 Å) (Figure 3c).

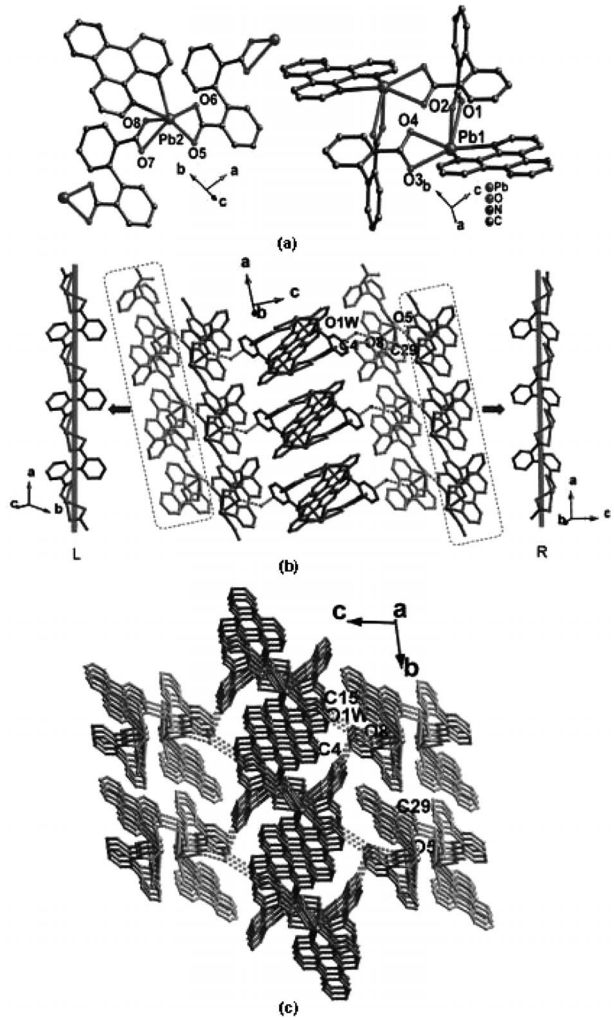

Figure 2. (a) Coordination environment for Pb^{II} ions in complex **2**. (b) 2D supramolecular network of **2** constructed by 1D left- / right-handed helical chains and dinuclear units through hydrogen bonding interactions. (c) 3D supramolecular architecture connected by hydrogen bonding interactions.

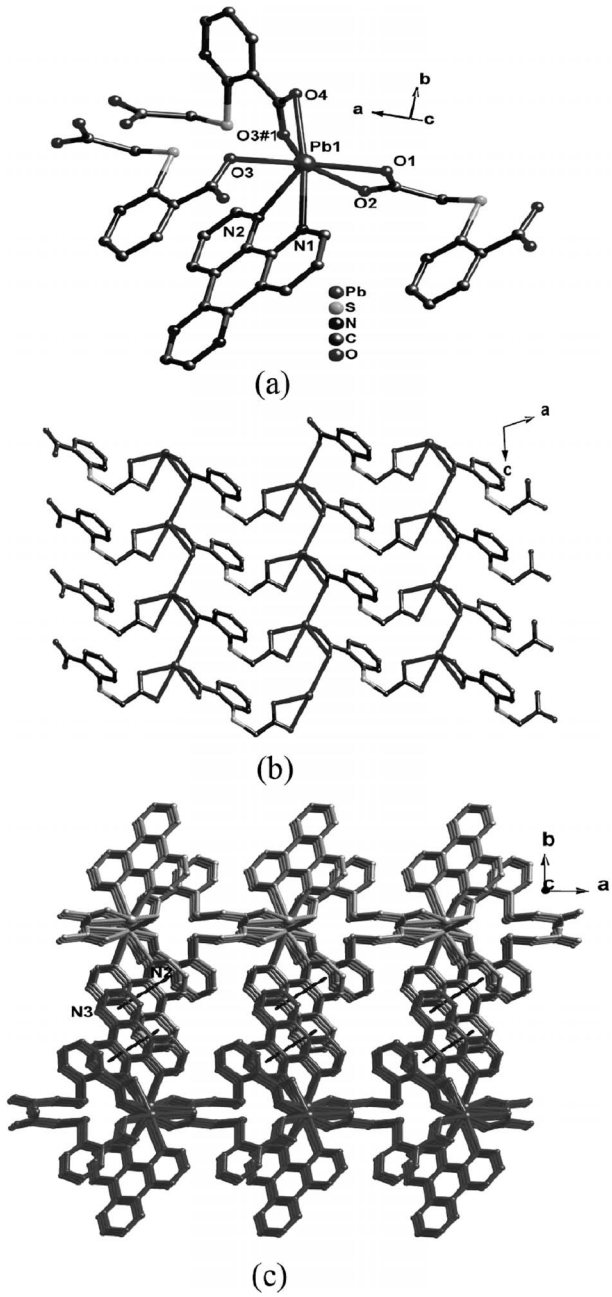

Figure 3. (a) Coordination environment for Pb^{II} ion in complex **3**. (b) 2D undulating network of **3** along *b* axis (dpq ligands are omitted for clarity). (c) 3D supramolecular architecture connected by π–π stacking interactions.

Pb^{II} coordination polymers based on N-donor chelating ligands and organic carboxylates have been prepared by some groups.[23,24] *Ma* and co-workers have obtained a 1D double chain complex $[Pb(pzp)(1,2\text{-bdc})]\cdot H_2O$ (pzp = pyrazino[2,3-f]-[1,10]phenanthroline, $1,2\text{-}H_2$bdc = benzene-1,2-dicarboxylic acid).[25] *Jin* et al. have reported a 1D left- and right-handed helical double-stranded complex [Pb(2-Hstp)(phen)] (phen = 1,10-phenanthroline, $2\text{-}NaH_2$stp = 2-sulfoterephthalate).[26] However, complex **3** presents the first lead complex derived from dpq and S-containing organic dicarboxylate.

Effect of the Central Metal and Dicarboxylates on the Structures of the Title Complexes

By tuning the coordination characters of the metal ions and the organic dicarboxylate ligands under the same conditions, we obtained three new metal-organic complexes with completely different architectures. In complexes **1** and **2**, the same chelating N-containing ligand (dpq) and organic dicarboxylate (L^1) were used. When a transition metal (Ni^{II}) was selected as the central metal in complex **1**, the L^1 anions exhibit two types of coordination modes: monodentate and bridging-bis(monodentate) modes (Scheme 2a), furnishing a semi-circling 0D dinuclear complex. The dihedral angles of the two phenyl rings from L^1 anion are 79.655° and 61.171°. However, in complex **2**, when a main group metal (Pb^{II}) was used, the L^1 anion only exhibited bis(chelating) bridging coordination mode (Scheme 2b), giving rise to a 0D + 1D cocrystal. The corresponding dihedral angles of L^1 anion are 76.755° and 63.534°, respectively. These may be attributed to the different coordination environment and arrangement of the central metal atoms in **1** and **2**. Comparing complex **2** with **3**, the effect of the carboxylates with different coordination sites and flexibilities on the architectures were clearly demonstrated. When L^1 anion is replaced by a flexible L^2 anion in complex **3**, the coordination number of the Pb^{II} atom increases from 6 in **2** to 7 in **3**, and the two carboxyl groups of L^2 anion show chelating and chelate-monodentate bridging coordination modes (Scheme 2c), respectively, resulting in a 2D coordination polymer.

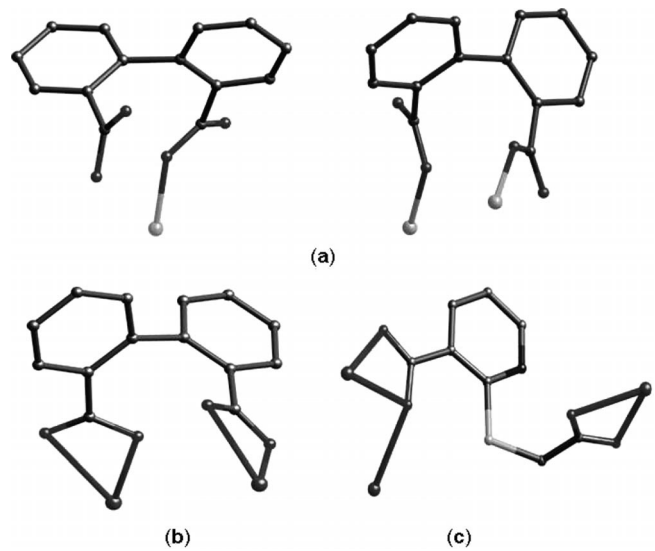

Scheme 2. The coordination modes of organic dicarboxylates in the title complexes.

IR Spectroscopy

The IR spectra of complexes **1**–**3** are shown in Figure S1 (Supporting Information). The bands around 735 cm^{-1} in complexes **1**–**3** may be attributed to the ν_{C-N} stretching of the pyrazinyl or pyridyl rings based on dpq ligand.[20] No strong ab-

Zeitschrift für anorganische und allgemeine Chemie ZAAC Journal of Inorganic and General Chemistry

sorption peaks around 1700 cm^{-1} for carboxyl groups were observed, indicating that all carboxyl groups of organic moieties in **1**–**3** are deprotonated.[27] The strong peaks at 1558, 1483, and 1391 cm^{-1} for **1**, 1597, 1539, and 1388 cm^{-1} for **2**, and 1583, 1539, and 1375 cm^{-1} for **3** may be attributed to the asymmetric and symmetric vibrations of carboxyl groups.[22] The strong broad band at around 3300 cm^{-1} was assigned to the ν(O–H) vibrations of coordinated and lattice water molecules in **1** and **2**.

Thermogravimetric Analysis (TGA)

To investigate the thermal stability of the title complexes, decomposition behavior of **1**–**3** were studied by thermogravimetric analyses (TGA) with a heating rate of 10 °C·min^{-1} in the temperature range of 20 to 780 °C (Figure S2, Supporting Information). The TG curve of **1** exhibits two weight loss stages in the range of 20–780 °C. The first weight loss of 9.89 % around 115–135 °C corresponds to the release of the coordinated and lattice water molecules (calcd. 9.74 %). The second weight loss in 300–600 °C was attributed to the decomposition of the framework with NiO as the final product (observed 12.54 %, calcd. 12.76 %).

Complex **2** also shows two weight loss steps. The first weight loss began at 20 °C and completed at 253 °C. The observed weight loss of 1.81 % is corresponding to the loss of the crystallization water molecules (calcd. 1.23 %). The second weight loss in 320–780 °C comes from the decomposition of the framework and the remaining weight corresponds to PbO (obs. 16.58, calcd. 16.21 %). The TGA curve of **3** shows a one step weight loss process from 243 to 430 °C, corresponding to the decomposition of organic components. PbO residue of 34.62 % (calcd. 34.30 %) is observed.

Photoluminescence Analyses

Luminescent complexes are of current interest because of their various applications in chemical sensors, photochemistry, and electroluminescent display.[28–30] In this paper, the solid state photoluminescent properties of complexes **1**–**3** were investigated at room temperature (Figure 4). Free dpq ligand displays a photoluminescent emission at 436 nm upon excitation at 360 nm in the solid state.[20] Complexes **1**–**3** exhibit fluorescent emission bands with maximum at 466, 533, and 457 nm, respectively, upon excitation at 340, 360 and 320 nm. Compared with that of the free ligand dpq, the emission peaks of **1**–**3** are red-shifted, which may be due to the intraligand fluorescent emission.[31] The different emission positions and intensities of **1**–**3** may be due to the significant difference of their structures and components, because the fluorescence behavior is closely associated with the metal ions and the ligands coordinated around them.[32,33]

Electrochemical Behavior of Complex 1 Bulk-modified Carbon Paste Electrode (1-CPE)

Figure 5 shows the cyclic voltammograms of a bare CPE and the **1**-CPE in 0.01 M H_2SO_4/0.5 M Na_2SO_4 aqueous solution at room temperature. It can be seen that in the potential range of +700 to –100 mV, there is no redox peak at the bare CPE. While the **1**-CPE exhibits one quasi-reversible redox peak and the mean peak potential $E_{1/2} = (E_{pa} + E_{pc})/2$ is approximately 324 mV (100 mV·s^{-1}), which could be attributed to the redox of Ni^{III}/Ni^{II}.[34–36]

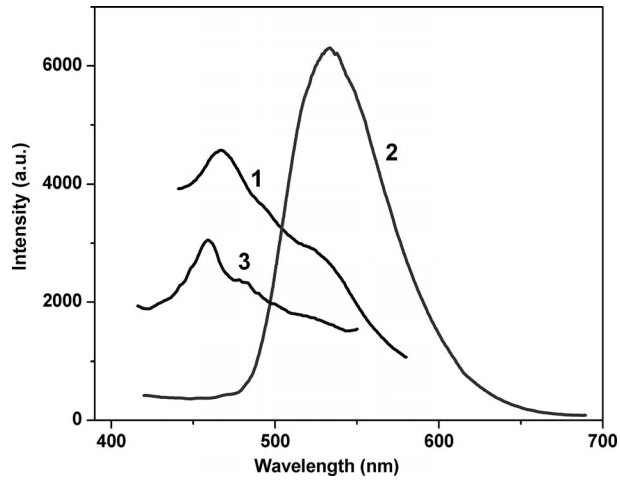

Figure 4. Fluorescence spectra for complexes **1**–**3** in the solid state at room temperature.

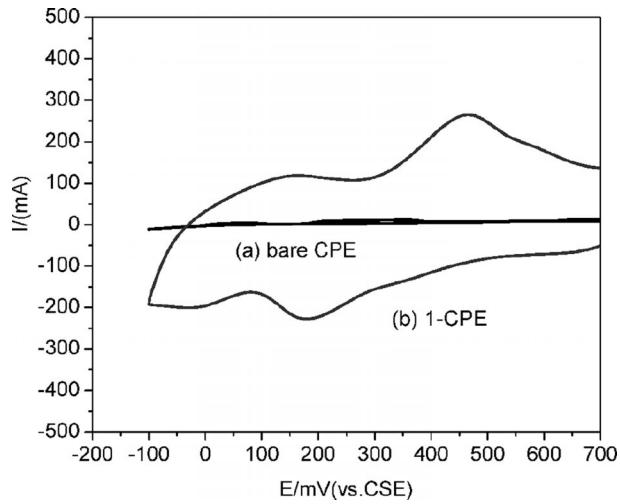

Figure 5. Cyclic voltammograms of (a) the bare CPE, (b) **1**-CPE in 0.01 M H_2SO_4/0.5 M Na_2SO_4 aqueous solution in the potential range of +700 to –100 mV. Scan rate: 100 mV·s^{-1}.

Figure 6 shows the cyclic voltammograms for the electrocatalytic reduction of nitrite at a bare CPE and the **1**-CPE in 0.01 M H_2SO_4/0.5 M Na_2SO_4 aqueous solution. There is no redox peak at the bare CPE in the presence of nitrite in the potential range of +700 to –100 mV. With the addition of nitrite, the reduction peak currents increase markedly while the corresponding oxidation peak currents decrease at the **1**-CPE. The results indicate that **1**-CPE has good electrocatalytic activity toward the reduction of nitrite.[37]

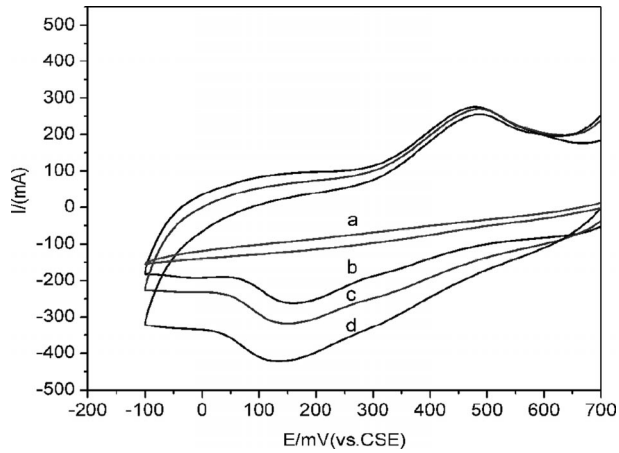

Figure 6. Cyclic voltammograms of (a) the bare CPE in 0.01 M H_2SO_4/0.5 M Na_2SO_4 solution containing 1.0 mmol L^{-1} KNO_2, (b–d) **1**-CPE in 0.01 M H_2SO_4/0.5 M Na_2SO_4 solution containing: 0.0, 2.0 and 4.0 mmol L^{-1} KNO_2. Scan rate: 100 mV·s^{-1}.

Conclusions

Three new 0D, 0D + 1D, and 2D metal-organic complexes were synthesized based on different metal ions and dicarboxylate anions. Complex **1** exhibits a semi-circling dinuclear complex, which is extended into a 3D supramolecular network by hydrogen bonding and π–π stacking interactions. Complex **2** features a 0D + 1D structure, which is ultimately packed into 3D supramolecular architecture through hydrogen bonding interactions. The differences of the frameworks between complexes **1** and **2** are mainly caused by the various coordination modes and atomic radius of the central metal atoms. So the appropriate selection of metal ions has significant effect on the formation and dimension of the resulting structures. Complex **3** shows a 2D sheet, which is extended into a 3D supramolecular framework by π–π stacking interactions. The structural differences of **2** and **3** are mainly due to the effect of the dicarboxylate with different coordination sites and flexibilities on the construction of the complexes. The successful preparation of complexes **1–3** provides a valuable approach for the construction of metal-organic complexes.

Experimental Section

Materials and Methods: H_2L^2 and dpq ligands were synthesized by literature methods.[38,39] All other chemicals purchased were of reagent grade and used without further purification. FT-IR spectra (KBr pellets) were taken with a Varian 640 FT-IR spectrometer in the 500–4000 cm^{-1} region. Elemental analyses were performed with a Perkin-Elmer 240CHN analyzer. Thermogravimetric data for the complexes **1–3** were collected with a Pyris Diamond thermal analyzer. Fluorescence spectra were performed with an F-4500 fluorescence/phosphorescence spectrophotometer at room temperature. UV/Vis absorption spectra were obtained with a SP-1900 UV/Vis spectrophotometer. The electrochemical properties were performed with a CHI 440 Electrochemical Quartz Crystal Microbalance. A conventional three-electrode cell was used at room temperature. The complex **1** bulk-modified carbon paste electrode (**1**-CPE) was used as working electrode. An SCE and a platinum wire were used as reference and auxiliary electrodes, respectively.

Synthesis of $[Ni_2(dpq)_2(L^1)_2(H_2O)_5]\cdot H_2O$ (1): A mixture of $NiCl_2\cdot 6H_2O$ (0.02 g, 0.1 mmol), H_2L^1 (0.02 g, 0.1 mmol), dpq (0.01 g, 0.05 mmol), H_2O (10 mL), and NaOH (0.01 g, 0.2 mmol) was stirred for 30 min in air, transferred to a 25 mL Teflon-lined stainless steel autoclave, and heated to 160 °C for 3 d. After the mixture was slowly cooled to room temperature, light green block crystals suitable for X-ray diffraction of **1** were obtained in 21% yield [based on Ni^{II} salt]. $C_{56}H_{44}N_8Ni_2O_{14}$: calcd. C 57.47, H 3.79, N 9.57%; found: C 57.61, H 3.59, N 9.28%. **IR** (KBr): $\tilde{\nu}$ = 3574 (s), 2898 (w), 2360 (s), 1699 (s), 1558 (m), 1541 (w), 1483 (m), 1390 (s), 1271 (m), 1126 (w), 1083 (m), 1051 (w), 818 (s), 758 (s), 736 (s), 673 (m), 563 (m) cm^{-1}.

Synthesis of $[Pb_2(dpq)_2(L^1)_2]\cdot H_2O$ (2): Similar procedure was performed to obtain yellow crystals of complex **2**, except that $Pb(NO_3)_2$ (0.03 g, 0.1 mmol) was used instead of $NiCl_2\cdot 6H_2O$. Yield: 25%. $C_{56}H_{34}N_8Pb_2O_9$: calcd. C 48.83, H 2.49, N 8.14%; found: C 48.72, H 2.61, N 8.32%. **IR** (KBr): $\tilde{\nu}$ = 3367 (s), 2359 (s), 1574 (s), 1539 (s), 1472 (m), 1389 (s), 1373 (w), 1340 (w), 1207 (m), 1150 (w), 1117 (w), 1080 (m), 1047 (w), 840 (m), 757 (s), 679 (m), 579 (w) cm^{-1}.

Synthesis of $[Pb(dpq)(L^2)]$ (3): The similar method to that for **2** was used except that H_2L^1 was replaced by H_2L^2 (0.02 g, 0.1 mmol), affording light yellow crystals of complex **3**. Yield: 17%. $C_{22}H_{13}N_5PbO_4S$: calcd. C 40.61, H 2.01, N 10.76%; found: C 40.42, H 2.23, N 10.59%. **IR** (KBr): $\tilde{\nu}$ = 3337 (m), 3053 (s), 1583 (s), 1562 (m), 1539 (w), 1473 (m), 1375 (s), 1217 (m), 1155 (w), 1080 (m), 1055 (w), 847 (s), 737 (s), 696 (m), 545 (w) cm^{-1}.

Preparations of Complex 1 Bulk-Modified Carbon Paste Electrode: Complex **1** bulk-modified carbon paste electrode (**1**-CPE) was fabricated by mixing complex **1** (0.01 g) and graphite powder (0.10 g) in an agate mortar for approximately 30 min to achieve an even, dry mixture; then paraffin oil (0.05 mL) was added and stirred with a glass rod. The homogenized mixture was packed into a 3 mm inner diameter glass tube and the tube surface was wiped with weighing paper. The electrical contact was established with the copper wire through the back of the electrode.

X-ray Crystallographic Study: X-ray diffraction data for complexes **1–3** were collected with a Bruker APEX-II CCD diffractometer equipped with graphite-monochromated Mo-K_α radiation with radiation wavelength 0.71073 Å by using the ϕ–ω scan technique at 296(2) K. The structures were solved by the direct method and refined by the Full-matrix least-squares on F^2 using the SHELXL software.[40,41] Non-hydrogen atoms were refined with anisotropic temperature parameters. The hydrogen atoms of organic ligands were generated geometrically and refined isotropically. Details for crystallographic data and structural analyses are summarized in Table 1, and selected bond parameters as well as hydrogen-bonding arrangements are listed in Tables S1–S4, respectively.

Crystallographic data (excluding structure factors) for the structures **1–3** in this paper have been deposited with the Cambridge Crystallographic Data Centre, CCDC, 12 Union Road, Cambridge CB21EZ, UK. Copies of the data can be obtained free of charge on quoting the depository numbers CCDC-902481, CCDC-902482, and CCDC-902483. (Fax: +44-1223-336-033; E-Mail: deposit@ccdc.cam.ac.uk, http://www.ccdc.cam.ac.uk)

Supporting Information (see footnote on the first page of this article): Selected bond lengths and angles for complexes **1–3**, hydrogen bond-

Zeitschrift für anorganische und allgemeine Chemie ZAAC Journal of Inorganic and General Chemistry

Table 1. Crystal data and structure refinements for complexes **1**–**3**.

	1	**2**	**3**
Formula	$C_{56}H_{44}N_8Ni_2O_{14}$	$C_{56}H_{34}N_8Pb_2O_9$	$C_{22}H_{13}N_5PbO_4S$
Formula wt.	1170.38	1377.31	650.64
Crystal system	triclinic	triclinic	monoclinic
Space group	$P\bar{1}$	$P\bar{1}$	$P2_1/c$
a /Å	10.2321(5)	8.2853(9)	9.2456(6)
b /Å	13.6627(7)	12.1093(13)	25.4229(16)
c /Å	19.2371(9)	24.649(2)	8.9168(6)
α /°	95.179(4)	98.443(8)	90
β /°	93.422(4)	91.263(9)	103.1630(10)
γ /°	103.090(4)	106.345(10)	90
V /Å^3	2599.8(2)	2342.1(4)	2040.8(2)
Z	2	2	4
D /g·cm^{-3}	1.495	1.953	2.118
μ /mm^{-1}	0.802	7.251	8.413
F(000)	1208	1324	1240
θ_{max} /°	25.000	25.15	25.00
Reflections collected	17296	16079	10342
Unique reflections	9144	8370	3587
R_{int}	0.0296	0.0449	0.0218
R_1[a)] [$I > 2\sigma(I)$]	0.0421	0.0395	0.0239
wR_2[b)] (all data)	0.1117	0.0926	0.0582
GOF	1.003	1.093	1.028
$\Delta\rho_{min}$ /e Å^{-3}	0.486	1.540	0.871
$\Delta\rho_{max}$ /e Å^{-3}	–0.555	–1.959	–1.258

a) $R_1 = \Sigma(||F_o|-|F_c||)/\Sigma|F_o|$. b) $wR_2 = [w(|F_o|^2-|F_c|^2)^2/(w|F_o|^2)^2]^{1/2}$.

ing parameters for complexes **1** and **2**, IR spectra and TG curves of complexes **1**–**3**, UV/Vis spectrum of complex **1**.

Acknowledgements

This work was financially supported by the National Natural Science Foundation of China (No. 21171025, 21201021), the Natural Science Foundation of Liaoning Province (No. 201102003) and the Program of Innovative Research Team in University of Liaoning Province (LT2012020).

References

[1] M. Eddaoudi, J. Kim, N. Rosi, D. Vodak, J. Wachter, M. O'Keeffe, O. M. Yaghi, *Science* **2002**, *295*, 469.
[2] J. S. Seo, D. Whang, H. Lee, S. I. Jun, J. Oh, Y. J. Jeon, K. Kim, *Nature* **2000**, *404*, 982.
[3] D. L. Reger, T. D. Wright, R. F. Semeniuc, T. C. Grattan, M. D. Smith, *Inorg. Chem.* **2001**, *40*, 6212.
[4] M. B. Zaman, M. D. Smith, H. C. Zur Loye, *Chem. Commun.* **2001**, *21*, 2256.
[5] J. Z. Gao, J. Yang, Y. Y. Liu, J. F. Ma, *CrystEngComm* **2012**, *14*, 8173.
[6] B. L. Chen, S. C. Xiang, G. D. Qian, *Acc. Chem. Res.* **2010**, *43*, 1115.
[7] B. Moulton, M. J. Zaworotko, *Chem. Rev.* **2001**, *101*, 1629.
[8] M. Eddaoudi, D. B. Moler, H. Li, B. Chen, T. M. Reineke, M. O'Keeffe, O. M. Yaghi, *Acc. Chem. Res.* **2001**, *34*, 319.
[9] G. M. Sun, H. X. Huang, X. Z. Tian, Y. M. Song, Y. Zhu, Z. J. Yuan, W. Y. Xu, M. B. Luo, S. J. Liu, X. F. Feng, F. Luo, *CrystEngComm* **2012**, *14*, 6182.
[10] X. L. Wang, Z. C. Guo, G. C. Liu, Y. Qu, S. Yang, H. Y. Lin, J. W. Zhang, *CrystEngComm* **2013**, *15*, 551.
[11] H. Li, M. Eddaoudi, M. O'Keeffe, O. M. Yaghi, *Nature* **1999**, *402*, 276.
[12] X. L. Sun, Z. J. Wang, S. Q. Zang, W. C. Song, C. X. Du, *Cryst. Growth Des.* **2012**, *12*, 4431.
[13] Z. B. Han, X. N. Cheng, X. M. Chen, *Cryst. Growth Des.* **2005**, *5*, 695.
[14] X. L. Wang, Y. F. Bi, H. Y. Lin, G. C. Liu, *Cryst. Growth Des.* **2007**, *7*, 1086.
[15] G. B. Che, C. B. Liu, B. Liu, Q. W. Wang, Z. L. Xu, *CrystEngComm* **2008**, *10*, 184.
[16] J. Y. Lu, V. Schauss, *Inorg. Chem. Commun.* **2003**, *6*, 1332.
[17] R. H. Wang, Y. F. Zhou, Y. Q. Sun, D. Q. Yuan, L. Han, B. Y. Lou, B. L. Wu, M. C. Hong, *Cryst. Growth Des.* **2005**, *5*, 251.
[18] X. R. Jiang, X. J. Wang, Y. L. Feng, *Inorg. Chim. Acta* **2012**, *383*, 38.
[19] X. X. Xu, Y. Lu, E. B. Wang, Y. Ma, X. L. Bai, *Cryst. Growth Des.* **2006**, *6*, 2029.
[20] X. L. Wang, Y. F. Bi, G. C. Liu, H. Y. Lin, T. L. Hu, X. H. Bu, *CrystEngComm* **2008**, *10*, 349.
[21] N. Liu, Q. Yue, Y. Q. Wang, A. L. Cheng, E. Q. Gao, *Dalton Trans.* **2008**, *34*, 4621.
[22] G. C. Liu, Y. Q. Chen, X. L. Wang, B. K. Chen, H. Y. Lin, *J. Solid State Chem.* **2009**, *182*, 566.
[23] C. Gabriel, C. P. Raptopoulou, V. Psycharis, A. Terzis, M. Zervou, C. Mateescu, A. Salifoglou, *Cryst. Growth Des.* **2011**, *11*, 382.
[24] X. L. Wang, Y. Q. Chen, Q. Gao, H. Y. Lin, G. C. Liu, J. X. Zhang, A. X. Tian, *Cryst. Growth Des.* **2010**, *10*, 2174.
[25] J. Yang, J. F. Ma, Y. Y. Liu, J. C. Ma, S. R. Batten, *Cryst. Growth Des.* **2009**, *9*, 1894.
[26] Y. X. Ren, X. J. Zheng, L. P. Jin, *CrystEngComm* **2011**, *13*, 5915.
[27] S. N. Wang, J. F. Bai, H. Xing, Y. Z. Li, Y. Song, Y. Pan, M. Scheer, X. Z. You, *Cryst. Growth Des.* **2007**, *7*, 747.
[28] K. H. He, W. C. Song, Y. W. Li, Y. Q. Chen, X. H. Bu, *Cryst. Growth Des.* **2012**, *12*, 1064.
[29] V. W. W. Yam, K. K. W. Lo, *Chem. Soc. Rev.* **1999**, *28*, 323.
[30] Y. J. Cui, Y. F. Yue, G. D. Qian, B. L. Chen, *Chem. Rev.* **2012**, *112*, 1126.
[31] X. Shi, G. S. Zhu, X. H. Wang, G. H. Li, Q. R. Fang, G. Wu, G. Tian, M. Xue, X. J. Zhao, R. W. Wang, S. L. Qiu, *Cryst. Growth Des.* **2005**, *5*, 207.
[32] J. C. Dai, X. T. Wu, Z. Y. Fu, C. P. Cui, S. M. Wu, W. X. Du, L. M. Wu, H. H. Zhang, Q. Sun, *Inorg. Chem.* **2002**, *41*, 1391.

[33] L. Y. Zhang, G. F. Liu, S. L. Zheng, B. H. Ye, X. M. Zhang, X. M. Chen, *Eur. J. Inorg. Chem.* **2003**, *16*, 2965.
[34] T. V. Mitkina, N. F. Zakharchuk, D. Y. Naumov, O. A. Gerasko, D. Fenske, V. P. Fedin, *Inorg. Chem.* **2008**, *47*, 6748.
[35] A. K. Singh, R. Mukherjee, *Dalton Trans.* **2005**, *17*, 2886.
[36] S. Pandey, P. P. Das, A. K. Singh, R. Mukherjee, *Dalton Trans.* **2011**, *40*, 10758.
[37] X. L. Wang, B. Mu, H. Y. Lin, G. C. Liu, *J. Organomet. Chem.* **2011**, *696*, 2313.
[38] X. J. Wang, Y. L. Feng, *Acta Crystallogr. Sect. E* **2010**, *66*, o1298.
[39] J. G. Collins, A. D. Sleeman, J. R. Aldrich-Wright, I. Greguric, T. W. Hambley, *Inorg. Chem.* **1998**, *37*, 3133.
[40] G. M. Sheldrick, *SHELXS-97*, Program for Crystal Structure Solution, Göttingen University, Germany, **1997**.
[41] G. M. Sheldrick, *SHELXS-97*, Program for Crystal Structure Refinement, Göttingen University, Germany, **1997**.

Received: January 8, 2013
Published Online: May 22, 2013

